

THS

This is to certify that the

dissertation entitled

MODEL ORDER REDUCTION FOR PLANE ELASTICITY USING EQUIVALENT MATERIAL DISTRIBUTION

presented by

Michael K. Penner

has been accepted towards fulfillment of the requirements for

M.S. degree in Mechanical Engineering

Date May 31, 2002

MSU is an Affirmative Action/Equal Opportunity Institution

0-12771

LIBRARY Michigan State University

PLACE IN RETURN BOX to remove this checkout from your record.

TO AVOID FINES return on or before date due.

MAY BE RECALLED with earlier due date if requested.

DATE DUE	DATE DUE	DATE DUE
		<u> </u>

6/01 c:/CIRC/DateDue.p65-p.15

MODEL ORDER REDUCTION FOR PLANE ELASTICITY USING EQUIVALENT MATERIAL DISTRIBUTION

BY

Michael K. Penner

A THESIS

Submitted to
Michigan State University
in partial fulfillment of the requirements
for the degree of

MASTER OF SCIENCE

Department of Mechanical Engineering

ABSTRACT

MODEL ORDER REDUCTION FOR PLANE ELASTICITY USING EQUIVALENT MATERIAL DISTRIBUTION

By

Michael K. Penner

A model order reduction technique is presented. This technique uses a multi-resolution analysis on a non-homogenous material distribution with fine scale features to construct a wavelet based reduced stiffness matrix. This reduced stiffness matrix is much smaller in size than fine scale stiffness matrix. A topology optimization technique is implemented to find a coarse, non-homogenous material distribution that has equivalent features to the reduced stiffness matrix. Results are presented for three different types of problems exhibiting different scales. The results show that fine scale materials can be represented by a coarse scale material distribution while keeping the elastic characteristics of the two systems approximately equal.

To my family and fiancée

ACKNOWLEDGEMENT

I would like to thank my advisor Prof. Alejandro Diaz for his guidance and patience, along with my committee, Professors Andre Benard and Farhang Pourboghrat. I would also like to thank Sudarsanam Chellappa for his support and direction in solving the problem.

TABLE OF CONTENTS

LIST OF FIGURES	vi
Chapter 1	
INTRODUCTION	1
Problem Statement	1
Chapter 2	
THE REDUCTION PROBLEM	7
Past Techniques	7
Wavelet Stiffness Matrix	12
Wavelet Stiffness Matrix	12
Chapter 3	
THE EQUIVALENT MATERIAL PROBLEM	16
Equivalent Material	16
Genetic Algorithm (GA)	
Chapter 4	
EXAMPLES	26
Scale 1 Solutions	31
Scale 2 Solutions	40
Scale 3 Solutions	49
Chapter 5	
CONCLUSIONS	57
Reference	59

LIST OF FIGURES

Figure 1.1 Unit square with non-homogenous material	2
Figure 1.2 Flow Chart of Numerical Process	5
Figure 2.1 Example of wavelet decomposition	14
Figure 3.1 Distribution of $\rho(x)$ computed using the 1 st technique to create initial population.	22
Figure 3.2 Distribution of $\rho(x)$ computed using the 2^{nd} technique to create initial population	23
Figure 3.3 Distribution of $\rho(x)$ computed using the 3^{rd} technique to create initial population	24
Figure 4.1 ¼ of material design	27
Figure 4.2 Symmetric material design	27
Figure 4.3 Geometry layouts for fine scale materials –Scale 1	28
Figure 4.4 Geometry layouts for fine scale materials –Scale 2	29
Figure 4.5 Geometry layouts for fine scale materials –Scale 3	30
Figure 4.6 Fine scale material distribution	32
Figure 4.7 Coarse scale material solution	32
Figure 4.8 9 th Mode shape from the target stiffness matrix	34
Figure 4.9 13 th Mode shape for the coarse material distribution	34
Figure 4.10 10 th Mode shape from the target stiffness matrix	35
Figure 4.11 14 th Mode shape from the target stiffness matrix	35
Figure 4.12 Fine scale material distribution	36
Figure 4.13 Coarse scale material distribution	36

Figure 4.14 5 th Mode shape from the target stiffness matrix	38
Figure 4.15 9 th Mode shape for the coarse material distribution	38
Figure 4.16 6 th Mode shape from the target stiffness matrix	39
Figure 4.17 10 th Mode shape for the coarse material distribution	39
Figure 4.18 Fine scale material distribution	40
Figure 4.19 Coarse scale material solution	40
Figure 4.20 3 rd Mode shape from the target stiffness matrix	42
Figure 4.21 4 th Mode shape for the coarse material distribution	42
Figure 4.22 10 th Mode shape from the target stiffness matrix	43
Figure 4.23 15 th Mode shape for the coarse material distribution	43
Figure 4.24 12 th Mode shape from the target stiffness matrix	44
Figure 4.25 21 st Mode shape for the coarse material distribution	44
Figure 4.26 Fine scale material distribution	46
Figure 4.27 Coarse scale material distribution solution	46
Figure 4.28 3 rd Mode shape from the target stiffness matrix	47
Figure 4.29 4 th Mode shape for the coarse material distribution	47
Figure 4.30 5 th Mode shape from the target stiffness matrix	48
Figure 4.31 5 th Mode shape for the coarse material distribution	48
Figure 4.32 Fine scale material distribution	49
Figure 4.33 Coarse scale material distribution solution	49
Figure 4.34 4 th Mode shape from the target stiffness matrix	50
Figure 4.35 3 rd Mode shape for the coarse material distribution	50
Figure 4.36 7 th Mode shape from the target stiffness matrix	51

Figure 4.37 7 th Mode shape for the coarse material distribution	51
Figure 4.38 9 th Mode shape from the target stiffness matrix	52
Figure 4.39 9 th Mode shape for the coarse material distribution	52
Figure 4.40 Fine scale material distribution	53
Figure 4.41 Coarse scale material solution	53
Figure 4.42 3 rd Mode shape from the target stiffness matrix	54
Figure 4.43 4 th Mode shape for the coarse material distribution	54
Figure 4.44 5 th Mode shape from the target stiffness matrix	55
Figure 4.45 7 th Mode shape for the coarse material distribution	55

Chapter 1

INTRODUCTION

With the need to increase the performance of a product, decrease design time and cost, the use of computer aided engineering techniques such as finite element methods are becoming ever more important. While this technique can be very effective on basic geometries and materials, its application is spreading to include more complex designs and materials including composites and foam like materials. This is causing the finite element model to become very complex and also increasing the computation time to solve these problems. This can have a negative effect on the design process, leaving some ideas unexplored due to the high computation time required. Also with the use of optimization programs that require the finite element computation to be done once per iteration, the time it takes to solve the problem gets multiplied. The goal of this thesis is to help develop model order reduction techniques that will decrease the complexity and size of the model and decrease the computation time while still keeping a high degree of accuracy of the solution.

1.1 Problem Statement

The reduction process discussed in this thesis begins with a plane elasticity problem on a unit square created with non-homogenous material as shown in Figure 1.1. In order to

resolve the details of the material distribution over the domain a fine scale resolution is needed.

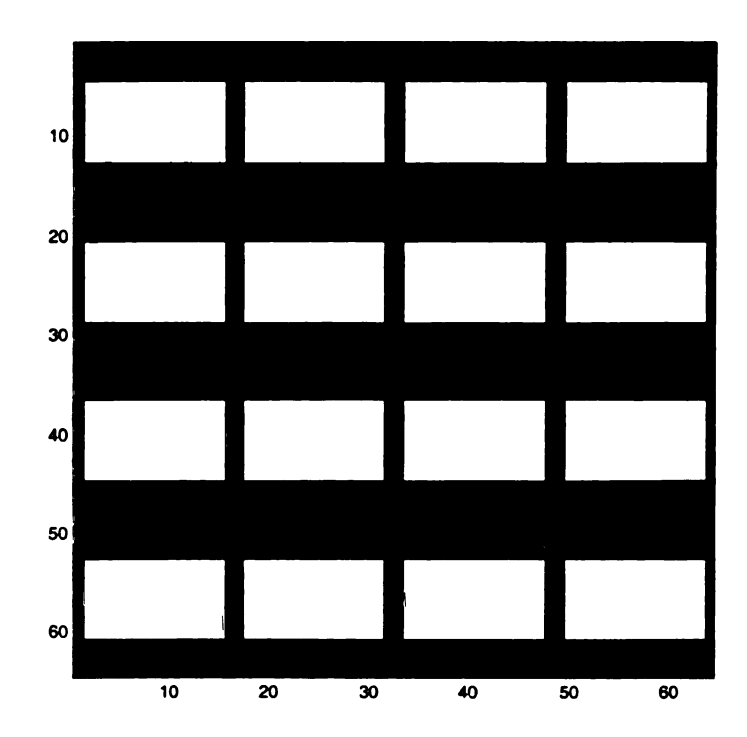


Figure 1.1 Unit square with non-homogenous material

The boundary conditions are periodic. Upon discretization and using wavelet Galerkin methods this problem can be expressed as

$$K_f^w u_f^w = F_f^w \tag{1}$$

where

 K_f^w is the fine scale wavelet stiffness matrix u_f^w is the fine scale wavelet coefficients F_f^w is the fine scale force wavelet coefficients

Equation (1) represents the fine scale problem. Since this process is based on a wavelet discretization, the degrees of freedom associated with the problem are wavelet coefficients.

Next, a reduction scheme based on a multi-resolution analysis (MRA) is applied to the fine scale problem. This procedure starts with the (very large) fine scale stiffness matrix (K_c^W) and creates a (much smaller) coarse scale stiffness matrix (K_c^W) . The boundary conditions remain periodic. The reduced system is

$$K_C^{\mathcal{W}} u_C^{\mathcal{W}} = F_C^{\mathcal{W}} \tag{2}$$

where

 K_c^w is the coarse scale wavelet stiffness matrix u_c^w is the coarse scale wavelet coefficients F_c^w is the coarse scale force wavelet coefficients

A transformation is now applied to the reduced wavelet stiffness matrix (K_c^W) to transform the wavelet degree of freedoms into nodal degrees of freedom. This procedure is just a coordinate transform. The result is a coarse scale stiffness matrix (K_c^n) where the degree of freedoms are now nodal displacements, not wavelet coefficients. Periodic boundary conditions still remain in force. This new reduced system is

$$K_C^n u_C^n = F_C^n \tag{3}$$

where

 K_c^n is the coarse scale nodal stiffness matrix u_c^n is the coarse scale nodal degree of freedom vector F_c^n is the coarse scale nodal degree of freedom vector

It should be noticed that matrix K_c^n , while it relates nodal degrees of freedom to nodal forces, it is not a finite element matrix.

The work in this thesis is to setup and solve an optimization problem to identify a coarse scale material distribution, E(x), on the unit square domain, such that the difference

$$||K_{c}(E(x)) - K_{c}^{nodal}||$$
 (4)

is minimized, where $K_C(E(x))$ is a standard finite element stiffness matrix. This problem is solved using a genetic algorithm, assuming that the material is isotropic and piecewise constant, i.e., $E(x) = \rho(x)E^0$ where $\rho(x) \in [0,1]$ is a piecewise constant function and E^0 is a fixed material tensor.

This process can be seen in the flow diagram below.

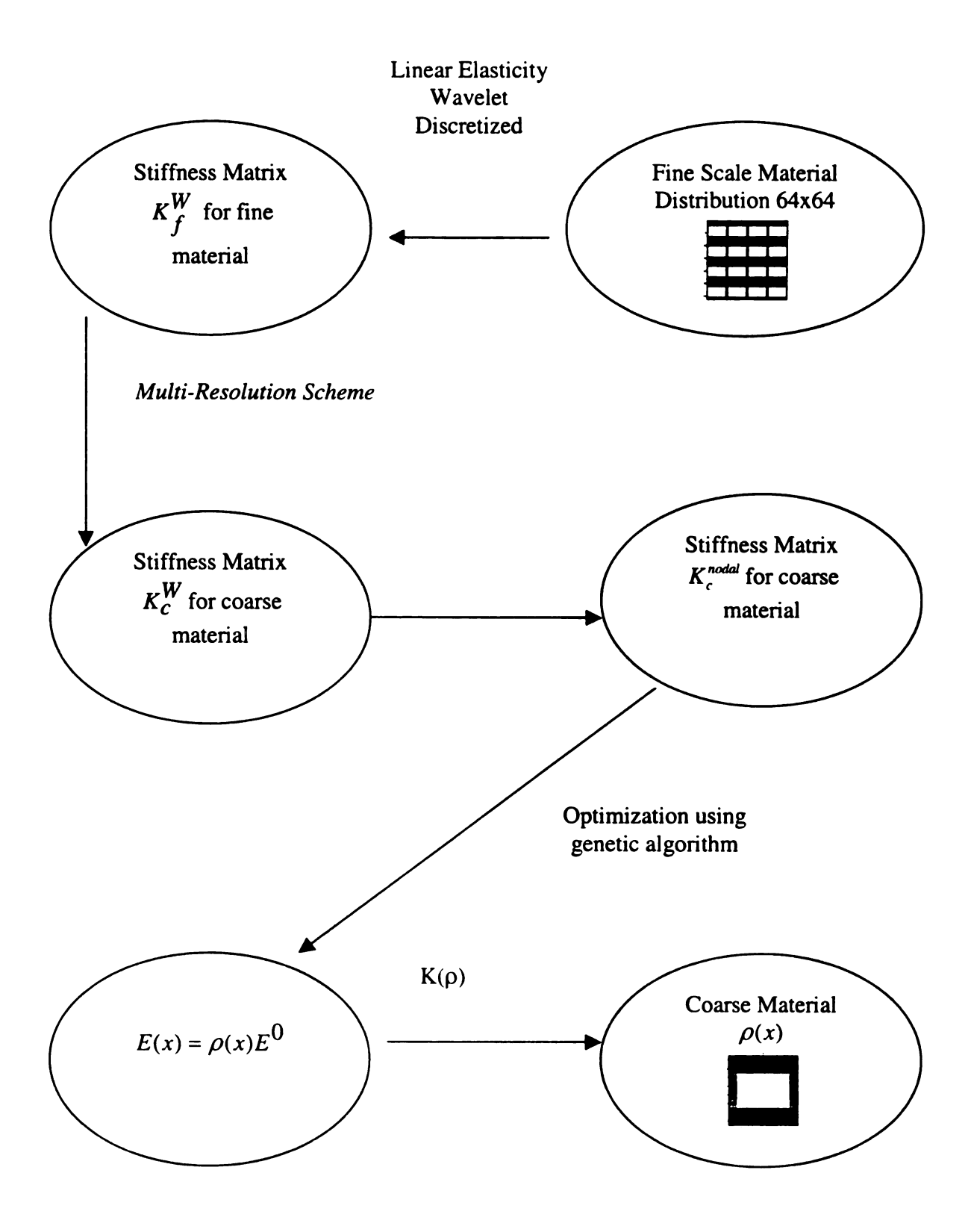


Figure 1.2 Flow Chart of Numerical Process

This thesis is divided into five chapters. The next chapter discusses in detail previous techniques of model order reduction and the technique used to create the reduced stiffness matrix used here. Chapter three talks about the equivalent material problem. Chapter four shows the numerical solutions and the methods to obtain these answers. The last chapter has the conclusions of this work.

Chapter 2

THE REDUCTION PROBLEM

2.1 Past Techniques

In this section common modeling order reduction techniques will be discussed, also the multi-resolution scheme used in this thesis will be shown.

(1) Static reduction. This is one of the simplest reduction methods. This process will neglect the inertia terms. This will only produce an exact result at a static condition or zero frequency. This can be seen in the following example taken from [3]. Start with the following linear system

$$\{F\} = [K]\{x\} \tag{2.1}$$

where

K is the stiffness matrix

F is a force vector

x is the nodal displacement vector

If [K] is symmetric

$$\begin{cases}
 F_1 \\
 F_2
 \end{cases} = \begin{bmatrix}
 K_A & B \\
 B^T & C
 \end{bmatrix} \begin{Bmatrix}
 x_m \\
 x_s
 \end{Bmatrix}$$
(2.2)

Assuming the F_2 to be zeros, solving for F_1 produces

$$F_1 = \left(A - BC^{-1}B'\right)x_m \tag{2.3}$$

with the reduced stiffness matrix being

$$K_1 = A - BC^{-1}B' (2.4)$$

This creates a coordinate transform, which is equal to

$$T = \begin{bmatrix} I \\ -C^{-1}B' \end{bmatrix} \tag{2.5}$$

which will yield the following reduced stiffness and mass matrices

$$K_1 = T'KT$$

$$M_1 = T'MT$$
(2.6)

If M is partitioned as

$$[M] = \begin{bmatrix} \overline{A} & \overline{B} \\ \overline{B} & \overline{C} \end{bmatrix} \tag{2.7}$$

the reduced mass matrix is

$$M_1 = \overline{A} - \overline{B}C^{-1}B' - \left(C^{-1}B'\right)\left(\overline{B}' - \overline{C}C^{-1}B'\right)$$
(2.8)

(2) Dynamic reduction. This is a modified version of the static reduction. This will produce an exact solution or response at a certain frequency. Selecting the correct frequency for the response is not apparent. The following process taken from Paz [5] outlines the procedure. Start with the eigenvalue problem in separated form

$$\begin{bmatrix}
[K_{SS}] - \omega^2[M_{SS}] & [K_{SP}] - \omega^2[M_{SP}] \\
[K_{PS}] - \omega^2[M_{PS}] & [K_{PP}] - \omega^2[M_{PP}]
\end{bmatrix} \begin{bmatrix} \{X_S\} \\ \{XP\} \end{bmatrix} = \begin{bmatrix} \{0\} \\ \{0\} \end{bmatrix}$$
(2.9)

where K is the stiffness matrix, M is the mass matrix, $\{X_s\}$ is the displacement or eigenvector corresponding to the s degree of freedoms to be reduced, $\{X_p\}$ are the corresponding p degree of freedoms to remain, and ω^2 is the approximate eigenvalue at each step. The first step is to assign a reasonable value to ω^2 for the first eigenvalue.

Then eliminate the first "s" displacements followed by elementary operations, at this point, equation (2.9) can be shown as

$$\begin{bmatrix} I \end{bmatrix} & \begin{bmatrix} -\overline{T} \end{bmatrix} \begin{bmatrix} \{X_s\} \\ [0] & [\overline{D}] \end{bmatrix} \begin{bmatrix} \{X_p\} \end{bmatrix} = \begin{bmatrix} \{0\} \\ \{0\} \end{bmatrix}$$
 (2.10)

with $[\overline{T}]$ as the transformation matrix that is defined in the following equation

$$\{X\} = \begin{Bmatrix} \{X_s\} \\ \{X_p\} \end{Bmatrix} = \begin{Bmatrix} [\overline{T}] \\ [I] \end{Bmatrix} \{X_p\}$$
 (2.11)

and $\left[\overline{D}\right]$ is the dynamic matrix that satisfies the equation

$$\left[\overline{K}\right] = \left[\overline{D}\right] + \omega^2 \left[\overline{M}\right] \tag{2.12}$$

 $[\overline{K}]$ is the reduced stiffness matrix and $[\overline{M}]$ is the reduced mass matrix which is found by the following equation

$$[\overline{M}] = [T]^T [M][T] \tag{2.13}$$

with [T] represented as

$$[T] = \begin{bmatrix} \overline{T} \\ I \end{bmatrix}$$
 (2.14)

The transformation $[\overline{T}]$ can be solved for, to obtain

$$\left[\overline{T}\right] = \left[-\left(K_{ss} - \omega_o^2 M_{ss}\right)^{-1} \left(K_{sm} - \omega_o^2 M_{sm}\right)\right]$$
 (2.15)

These expressions will lead to the equation

$$\left[\left[\overline{K}\right] - \omega^2 \left[\overline{M}\right]\right] \left\{X_n\right\} = \left\{0\right\} \tag{2.16}$$

Solving this equation will lead to an almost exact value of the first natural frequency and eigenvector. The second eigenvalue will be a close approximation. By inserting this close approximation value into the first equation and repeating the steps above, the output

will be a near exact solution for the second eigenvalue. This process can be repeated to produce near exact solutions for the eigenvalues and eigenvectors for the lowest p values [5].

(3) Improved reduction system. This technique builds off the static condition by including the inertia terms as psuedo static forces. This can be seen in the following example taken from [6] and [7]. Start with the equations of motion assembled in the following manner similar to the static condition

$$\begin{bmatrix} M_{mm} & M_{ms} \\ M_{sm} & M_{ss} \end{bmatrix} \begin{bmatrix} \ddot{x}_m \\ \ddot{x}_s \end{bmatrix} + \begin{bmatrix} K_{mm} & K_{ms} \\ K_{sm} & K_{ss} \end{bmatrix} \begin{bmatrix} x_m \\ x_s \end{bmatrix} = \begin{bmatrix} f_m \\ 0 \end{bmatrix}$$
 (2.17)

This expresses the mass [M] and stiffness [K] matrices ordered in terms of master and slave degrees of freedom. The master (m) degrees of freedom represent the retained values while the slave (s) degrees of freedoms represent the discarded values. Also assume that there are no forces applied to the slave degrees of freedom.

Neglecting inertia terms in the second equation set

$$\begin{Bmatrix} x_m \\ x_s \end{Bmatrix} = \begin{bmatrix} I \\ -K_{ss}^{-1}K_{sm} \end{bmatrix} x_m = T_s x_m$$
 (2.18)

 T_s represents the static transformation from the full state vector to that of a master coordinates. The reduced mass and stiffness matrices can be shown as

$$M_R = T_s^T M T_s$$

$$K_R = T_s^T K T_s$$
(2.19)

This is where the improved reduction system follows a different path than that of the static reduction. This is done by including the inertia terms as pseudo-static forces in the

transformation from the static case. This will allow the reduced model to represent the full model in low frequency responses. The improved reduction system starts with

$$T_{IRS} = T_s + SMT_s M_R^{-1} K_R (2.20)$$

where

$$S = \begin{bmatrix} 0 & 0 \\ 0 & K_{ss}^{-1} \end{bmatrix} \tag{2.21}$$

The reduced mass and stiffness matrices are

$$M_{IRS} = T_{IRS}^{T} M T_{IRS}$$

$$K_{IRS} = T_{IRS}^{T} K T_{IRS}$$
(2.22)

(4) System equivalent reduction expansion process (SEREP). The SEREP process utilizes eigenvectors to help deicide which nodes are kept. This method will produce exact answers for lower natural frequencies [7]. The next few steps will outline the procedure required to the reduction technique. First define the transformation noting that the numbers of master degrees of freedom are more than that of the modes of interest.

$$T = \begin{bmatrix} \Phi_m \\ \Phi_s \end{bmatrix} \left[\Phi_m^T \Phi_m \right]^{-1} \Phi_m^T \tag{2.23}$$

 Φ_m and Φ_s are the modes of interest at the master and slave degrees of freedom. Allowing the number of the numbers of master degrees of freedom to equal that of the modes of interest the equation above can be simplified to result the following transformation equation

$$T = \begin{bmatrix} \Phi_m \\ \Phi_s \end{bmatrix} \Phi_m^{-1} \tag{2.24}$$

Substituting equation (2.31) into IRS equation and applying to the transformation to Φ_m , gives

$$T\Phi_{m} = \begin{bmatrix} I \\ -K_{ss}^{-1}K_{sm} \end{bmatrix} \Phi_{m} + \begin{bmatrix} 0 & 0 \\ K_{ss}^{-1} & I \end{bmatrix} \begin{bmatrix} \Phi_{m} \\ \Phi_{s} \end{bmatrix} = \begin{bmatrix} \Phi_{m} \\ \Phi_{s} \end{bmatrix}$$
(2.25)

All these methods have one goal: to be able reduce the finite element model and keep the results accurate. By reducing the model, the computation time is decreased allowing for quicker results. Some of these techniques have been developed for specific set of problems while others have been developed for use on a broad spectrum of problems. The next section will discuss the techniques used in part by this thesis to create the reduced stiffness matrix.

2.2 Wavelet Stiffness Matrix

Let Ω be a domain occupied by a linearly elastic material, a square of size $2^J \times 2^J$ with J>0 as a fixed integer that represents the level of discretization. Ω is occupied by two different materials. Let $\rho(x)$ represent a piecewise constant function describing the material distribution within Ω . Let the material distribution within Ω be of the form

$$E(x) = \rho(x) \cdot E^{O} \tag{2.26}$$

where

$$E^{o} = \begin{bmatrix} E_{1111} & E_{1122} & 0 \\ E_{1122} & E_{2222} & 0 \\ 0 & 0 & E_{1212} \end{bmatrix} \qquad E_{1111} = \frac{E}{1 - v^{2}} \qquad E_{1122} = \frac{E \ v}{1 - v^{2}}$$

$$E_{2222} = \frac{E}{1 - v^{2}} \qquad E_{1212} = \frac{E \ (1 - v)}{1 - v^{2}}$$

(2.27)

where E is the modulus of elasticity, v is the Poisson's ratio and $\rho \in [0,1]$ is piecewise constant over the pixels [i,i+1]x[j,j+1].

Upon discretization and applying wavelet Galerkin techniques, the equilibrium equations become

$$K_f^w u_f^w = F_f^w \tag{2.28}$$

where

 K_f^w is the (fine scale) wavelet stiffness matrix at level J u_f^w are the (fine scale) vector of displacement wavelet coefficients

 F_f^w are the (fine scale) vector of force wavelet coefficients

Here we will describe a multi-resolution process that was developed by Diaz and Chellappa [4]. Readers are encouraged to read this and other papers in the reference for more details and insights into the multi-resolution process proposed here. Start with equation (2.28):

$$K^J u^J = F^J (2.29)$$

where the new notation emphasizes the scale, i.e. operator K^J is the stiffness matrix at level J. u^J is the displacement coefficients at level J and F^J is the force coefficients at level J. In two-dimensional elasticity u^J is a vector of size $(2*2^{2*J})$.

Using a wavelet transformation W we decompose the displacement (signal) u^J into a coarse component at scale J-1 (u^{J-1}) and a orthogonal complement of details at scale J-1 (u^{J-1})

$$W: u^J \to u^{J-1} \oplus w^{J-1} \tag{2.30}$$

An example of this transformation can be seen in figure 2.1.

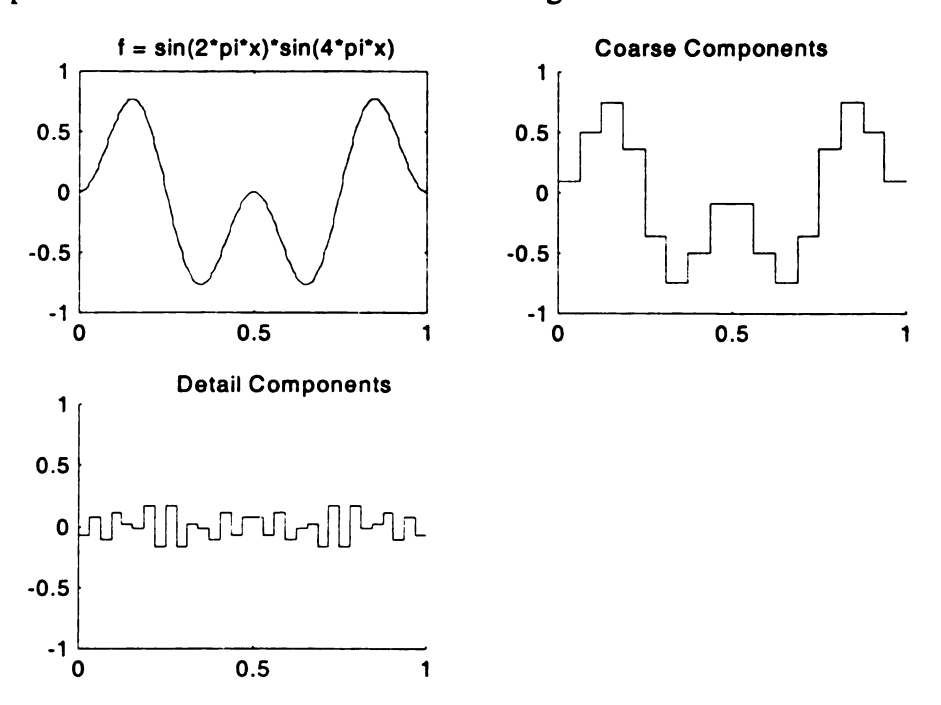


Figure 2.1 Example of wavelet decomposition

Now equation (2.29) can be written as

$$\begin{bmatrix} K^{J-1} & B^T \\ B & C \end{bmatrix} \begin{bmatrix} u^{J-1} \\ w^{J-1} \end{bmatrix} = \begin{bmatrix} f^{J-1} \\ g^{J-1} \end{bmatrix}$$
 (2.31)

 f^{J-1} and g^{J-1} are the coarse scale and detail components of the force. One should note that equation (2.31) is similar to that of the static reduction (equation (2.2)) shown at the beginning of the chapter. The only difference is that the master and slave degree of freedoms shown in equation (2.31) are decided here by separating the detail and coarse scales of the solution. Solving for the coarse scale problem will yield

$$\overline{K}^{J-1}u^{J-1} = F^{J-1} \tag{2.32}$$

where \overline{K}^{J-1} is

$$\overline{K}^{J-1} = K^{J-1} - B^T C^{-1} B \tag{2.33}$$

This process can be repeated to give the operator \overline{K}^{J-1} at any reduced scale.

Chapter 3

THE EQUIVALENT MATERIAL PROBLEM

3.1 Equivalent Material

Let $\rho(x)$ represent a piecewise constant function describing the material distribution within the domain Ω where $\rho(x) \in [0,1]$. The material tensor for each element in Ω is defined as

$$E(x) = \rho(x)E^{0} \tag{3.1}$$

where E^0 is a fixed tensor of elastic properties. The finite element stiffness matrix (K) is created using the material distribution $\rho(x)$, i.e.

$$K(\rho(x))u = f \tag{3.2}$$

where

 $K(\rho(x))$ = the finite element stiffness matrix

u = the finite element nodal displacement vector

f = the finite element force vector

It should be noted that the material distribution within Ω will vary from element to element. The stiffness matrix in equation (3.2) is called here the finite element stiffness matrix.

Starting with equation (2.32) from the last chapter

$$\overline{K}u = F \tag{3.3}$$

This (\overline{K}) is a reduced matrix at scale J-1. \overline{K} relates wavelet (coefficients) degrees of freedom to wavelet (coefficient) forces. We now set out to find an equivalent finite element matrix. To achieve this, first we must convert \overline{K} to a matrix that relates nodal displacements to nodal forces. Such matrix, K^n is of the form

$$K^{n} = B(r)^{T} \overline{K}^{J-1} B(r)$$
(3.4)

where

 $r = \{r_1, r_2, ..., r_n\}$ is a coarse scale material distribution

The stiffness matrix K^n from equation (3.4) is called here the target stiffness matrix.

This matrix is the same dimension as the reduced wavelet matrix from equation (2.33).

The matrix (B) is such that if u^w is a vector of wavelet coefficients, which results in a strain field $\varepsilon(u^w)$, B u^w is a vector of nodal forces associated with this pre-strain, ie, B is a (global) strain-displacement matrix.

The effective density for the fine scale and coarse scale problem can be defined as

$$effd = \frac{1}{e} \left(\sum_{1}^{N_e} \rho(x_e) \right)$$
 (3.5)

where N_e is the number of elements

Here the effective density for the fine scale and coarse scale problems are called effd_{fine} and effd_{coarse} respectively.

The objective of the equivalent material problem is to minimize the difference between the topology finite element stiffness matrix $(K(\rho))$ and the target stiffness matrix. This can be set up so that the energies of the two systems can be compared.

Find:
$$\rho_e = {\rho_1, \rho_2, \dots \rho_n}$$

Minimize:
$$f(\rho)$$

Subject to:
$$x_{\text{lower bound}} \le \rho_{\epsilon} \le x_{\text{upper bound}}$$

$$effd_{fine} \approx effd_{coarse}$$

The objective function is defined as

$$f(\rho) = \sum_{i} (\Phi_{i}^{T} K^{n} \Phi_{i} - \Phi_{i}^{T} K (\rho) \Phi_{i})^{2} + \|A - diag(A)\|_{Frobenius}$$

where

$$A = \Psi^{T}(K^{n} - K(\rho))\Psi$$

 Ψ = matrix of size (m, 2 * 2^{2*j}) with the iths eigenvectors

 Φ_i = is the ith eigenvector of K^n

m = dimension(i)

This problem is solved using a genetic algorithm. This method of solving was chosen over other gradient-based methods, this was because the gradient-based methods were too dependent on the staring guess. This means that the solutions from the gradient-based methods were finding local minimums instead of global minimums. The genetic algorithm was setup to maximize the fitness or the inverse of the objective function.

3.2 Genetic Algorithm (GA)

dependent on the staring guess. This means that the solutions from the gradient-based methods were finding local minimums instead of global minimums. The genetic algorithm was setup to maximize the fitness or the inverse of the objective function.

3.2 Genetic Algorithm (GA)

The genetic algorithms start with an initial population and employ the idea that only the fittest members of the population will reproduce and make it to the next generation. The evaluation or fitness of each member of the population is based on a function that is created and is specific to the problem. The following summarized outline of a GA program is shown below to illustrate the ideas mentioned here [13].

```
generate initial population, G(0)

evaluate G(0)

t=0

repeat

t=t+1

generate G(t) from G(t-1)

evaluate G(t)

until solution is found
```

This process is repeated until a solution that is fit enough is found.

There are six major components that make up a genetic algorithm [14]. They are chromosome representation, selection function, genetic operators making up the reproduction function, the creation of the initial population, termination criteria and finally the evaluation function. They will be listed here and discussed in detail.

1. Chromosome Representation

This how each individual member of the population is represented and this will determine how the GA is setup. This representation could be in many formats

including binary digits, floating-point numbers, integers, symbols, matrices, etc. Much work has been done [Michalewicz 1994] comparing the performance between different representations. In Michalewicz [Michalewicz 1994] it is shown that floating-point numbers between the lower and upper bounds give quicker and better results. This is the technique that was used in this research.

2. Selection Function

This will determine which and how many individuals contribute to the successive generations. Based on performance a probabilistic selection is done with the better-fit individuals having a better chance to get selected. The method used here is a ranking selection function based on the normalized geometric distribution. Ranking methods only need to map the solutions of a partially ordered set. The normalized geometric ranking methods can be seen as

$$P[\text{selecting the ith individual }] = q'(1-q)^{r-1}$$

with

q = the probability of selecting the best individual

r =the rank of the individual, where 1 is the best

P =the population size

$$q' = \frac{q}{1 - (1 - q)^{P}}$$

3. Genetic Operators

There are many crossover techniques used in GA's these include simple crossover, arithmetic crossover and heuristic crossover. The technique implemented in this thesis was an arithmetic crossover and will be explained below.

The arithmetic crossover produces two complimentary linear combinations of the "parents".

Mutation techniques can take on many forms. The technique used in this research was non-uniform mutation.

4. Creation of the Initial Population

In most applications the initial population is created from a random set of values with in the bounds of the problem. Once this is done the initial population gets evaluated and the fitness of each member is then used to start the GA. Many techniques can be implemented to create the initial population. This research used a three-part technique to create the population.

The initial population was created using three different techniques. The first technique creates the maximum number of black elements allowed by comparing it to the effective density of the fine scale. An element is defined as one entry in ρ_e . A black element means that the entry will have a value of one. Once this is done the black elements are then scaled down to achieve the actual effective density.

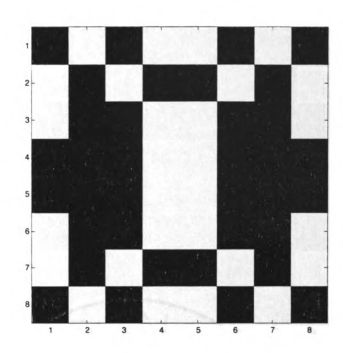


Figure 3.1 Distribution of $\rho(x)$ computed using the 1st technique to create initial population.

The second technique is a random distribution over all elements. If the effective density of the random solution is below the prescribed effective density, the elements with lower values are scaled up. If the density of the random solution is above the effective density the elements with higher values are scaled down, this uses an iteration technique to get the correct effective density.

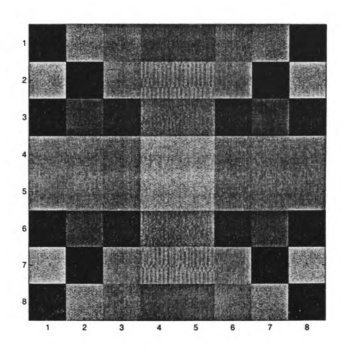


Figure 3.2 Distribution of $\rho(x)$ computed using the 2^{nd} technique to create initial population

The third technique (figure 3.3) involves using the images similar to that of the reduced wavelet transform of the fine scale material distribution. These images are created from taking the reduced wavelet transform of the fine scale material distribution and adding noise as seen in the following figure.

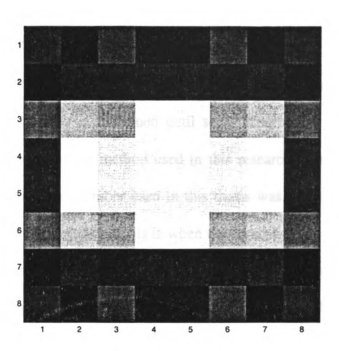


Figure 3.3 Distribution of $\rho(x)$ computed using the 3rd technique to create initial population

This is done to partially seed the initial population. The density of this solution is also equal to that of the effective density. Each of these three parts contributes equally to the creation of the initial population. The initial population was created using 85,000 members. This value was obtained from a trade off between size and the time it took to solve the problem. Values calculated above this value yielded little better results but increased the computation time.

5. Termination Function

The GA operates by evaluating all the members in a population, creating a new population. This process is continued until some criteria are met. The usual termination function (and the method used in this research) is the maximum of generations allowed. The number used in this thesis was 65. Other techniques include population convergence. This is when the sum of the deviations between fitness values of members of the population becomes less then some specified number, then the generations are terminated. The technique of terminating the sequence after 65 generations was used instead of the population convergence because of wanting to keep all the problems in the library consistent.

6. Evaluation Function

This is the function that evaluates the fitness of each member of the population. This is done by using the objective function defined at the beginning of the chapter. The fitness is defined as the inverse of the objective function. This done because GAs aim to increase the fitness level, so by taking the fitness as being the inverse of the objective function, it will be minimized.

Chapter 4

EXAMPLES

This chapter illustrates the use of the model order reduction technique developed in the previous chapters. In these examples the fine scale material distribution of different geometries is present in the figures along with the coarse scale material distribution solution. In all the examples cited the fine scale material is resolved by a 64x64 pixel distribution, with the coarse scale distribution representing 8x8 pixel grid. As stated before this represents three levels of reduction. In all cases the black material represents the following elastic material tensor

$$E_{black} = \begin{bmatrix} .91 & .3 & 0 \\ .3 & .91 & 0 \\ 0 & 0 & .769 \end{bmatrix}$$
 (4.1)

and white material tensor shown as

$$E_{white} = \begin{bmatrix} 91e - 6 & .3 & 0 \\ .3 & 91e - 6 & 0 \\ 0 & 0 & 70e - 6 \end{bmatrix}$$
 (4.2)

The gray material is a linear interpolation between these two bounds.

For all the problems shown here a symmetry constraint was introduced. This constraint was introduced because the fine scale material distribution had symmetry about the x and y axis. Only allowing ¼ of the design domain space to be solved and then duplicating or

repeating that area to fill in the rest of the design space accomplished the symmetry constraint. This can be seen in figures (4.1) and (4.2).



Figure 4.1 1/4 of material design

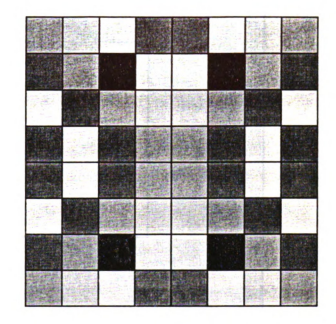


Figure 4.2 Symmetric material design

As stated before these examples were obtained by implementing a Genetic Algorithm [14] technique to solve the inverse homogenization problem for the reduced stiffness matrix. The details of these calculations are shown in the previous chapters. The rest of this chapter will be divided into three sections, each section devoted to each one of the scales. The geometries are laid out as shown in figure 4.3 for the first scale, figure 4.4 for the second and figure 4.5 for the third scale.

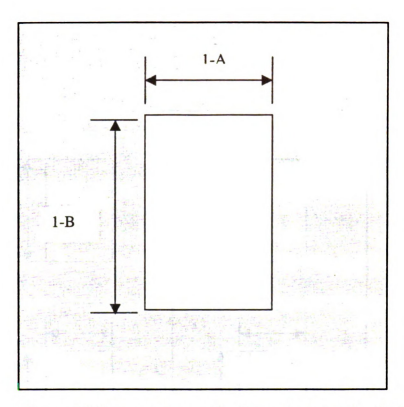


Figure 4.3 Geometry layouts for fine scale materials -Scale 1

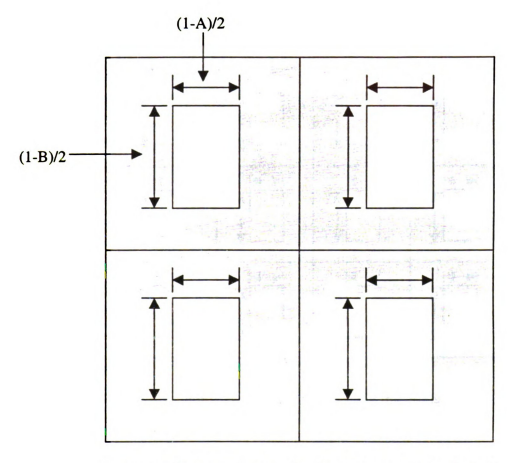


Figure 4.4 Geometry layouts for fine scale materials –Scale 2

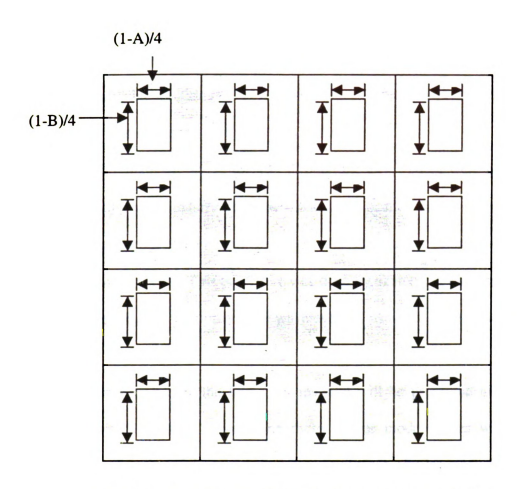


Figure 4.5 Geometry layouts for fine scale materials -Scale 3

The values of A and B vary depending on the scale that they are on. This can be seen in the table list below.

Scale	Starting Value	Ending Value	Increment
1	0	1	1/8
2	0	1	1/16
3	0	1	1/32

Table 4.1 Values of A and B for the three scales

4.1 Scale 1 Solutions

The fine scale picture and coarse scale picture are shown in figures 4.6 and 4.7. The fitness of this particular solution is shown to be 1.171. This represents a solution is 1.171 times better than that of the wavelet transform of the fine scale picture. The eigenvectors that contributed to this solution are the 13th through the 28th. These were picked so that they exhibit the fine scale features of figure 4.6 and the location of movement was not in an node that was surrounded by weak material. The rigid body mode shapes were not included in the calculations. This procedure was done by examining each mode shape of the reduced finite element solution and the wavelet transform of the fine scale material.

For the examples shown here the fine scale material will be presented along with the coarse scale material solution. Following these figures mode shapes will be shown demonstrating the fact that if the two systems are equivalent, similar mode shapes should appear at approximately the same frequency.

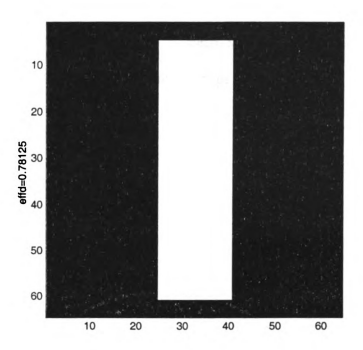


Figure 4.6 Fine scale material distribution

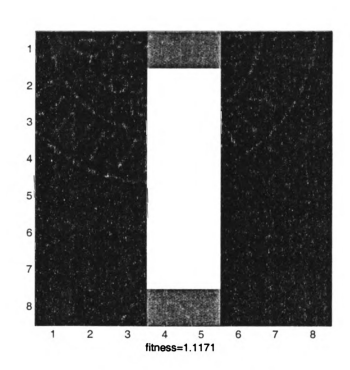


Figure 4.7 Coarse scale material solution

The following figures will demonstrate the accuracy of the solution above. This is done by showing that certain mode shapes of each solution and noting that the energy (eigenvalue) associated with that deformation shape is about equal.

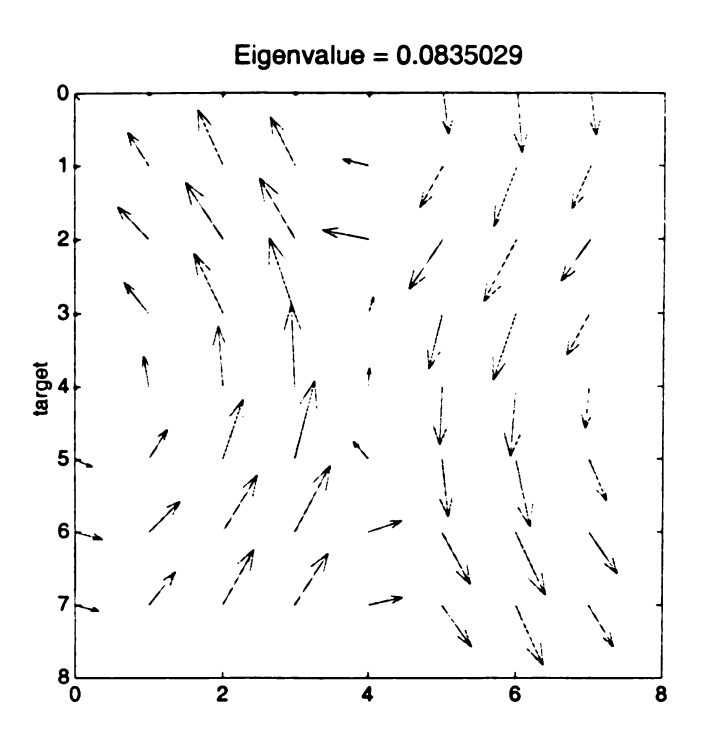


Figure 4.8 9th Mode shape from the target stiffness matrix

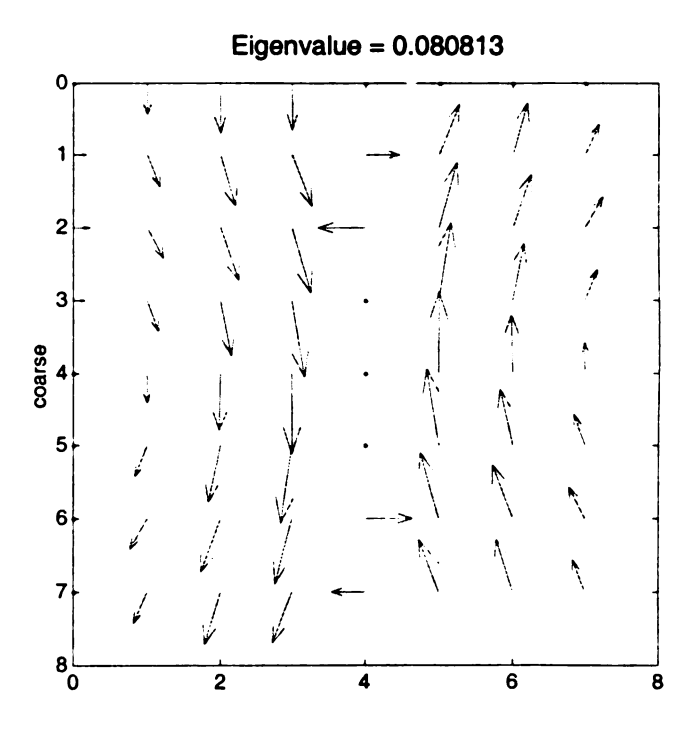


Figure 4.9 13th Mode shape for the coarse material distribution

As seen in figures (4.8) and (4.9) the mode shape deformations are qualitatively the same, with the eigenvalues about equal. The following figures will demonstrate this point for more mode shapes.

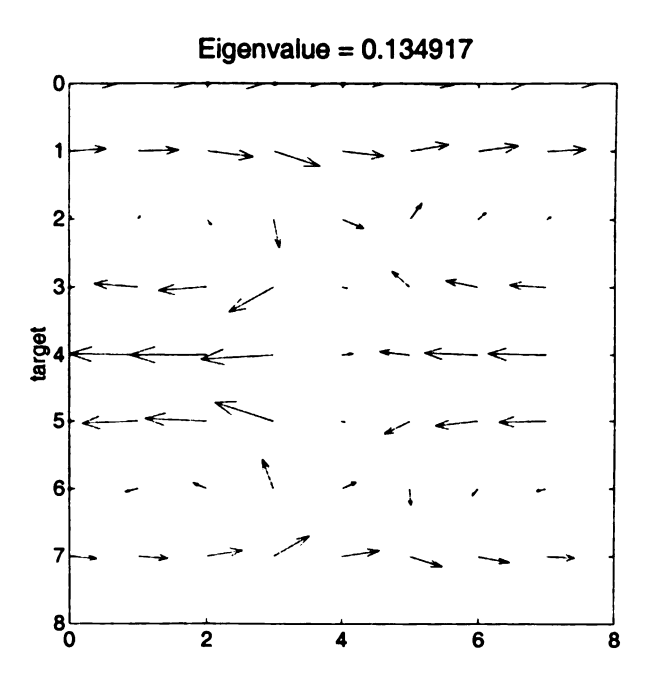


Figure 4.10 10th Mode shape from the target stiffness matrix

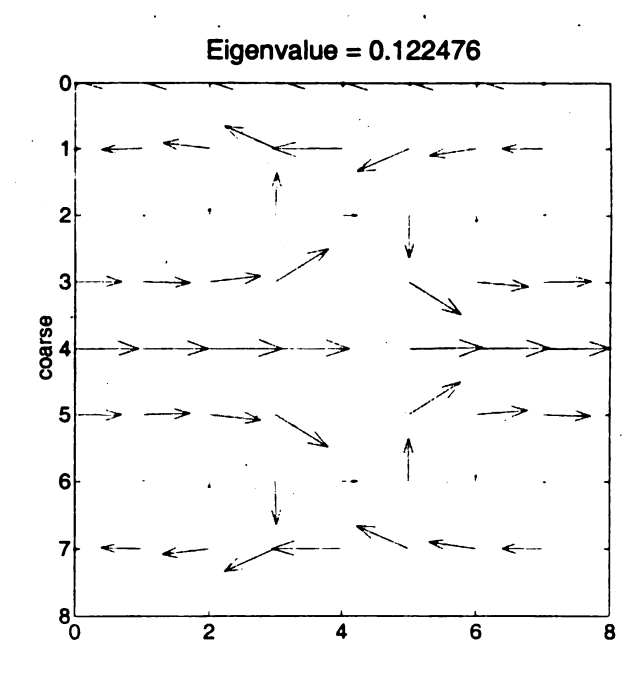


Figure 4.11 14th Mode shape from the target stiffness matrix

Another example of scale one solution.

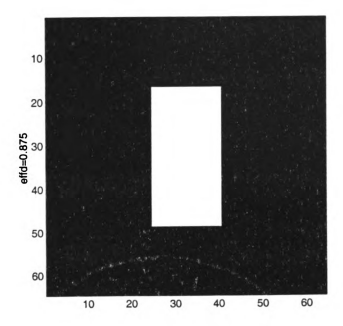


Figure 4.12 Fine scale material distribution

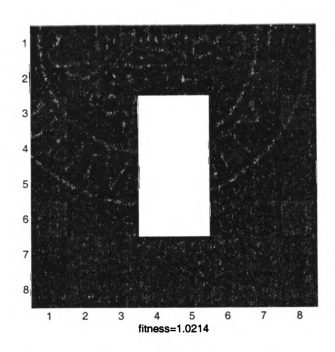


Figure 4.13 Coarse scale material distribution

Readers should note that the fine and coarse scale material distributions are very similar. This is because the values of A and B correspond exactly to the wavelet transform of the reduced material. Again noting the similarity between the energies of the two systems at deformed shapes.

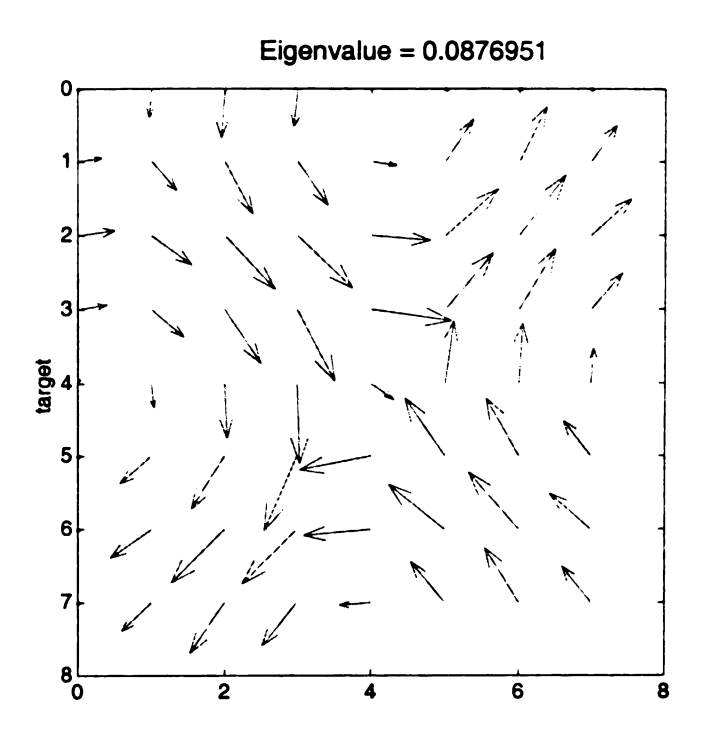


Figure 4.14 5th Mode shape from the target stiffness matrix

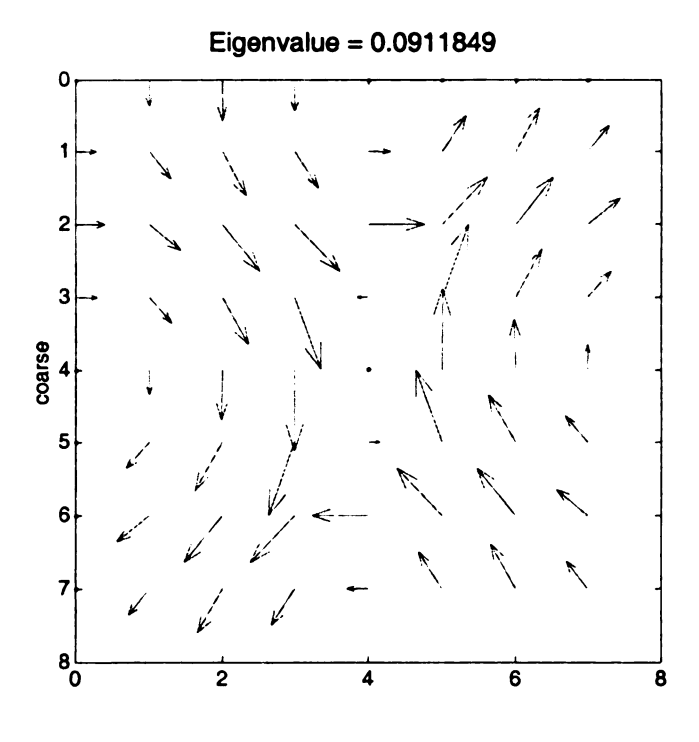


Figure 4.15 9th Mode shape for the coarse material distribution

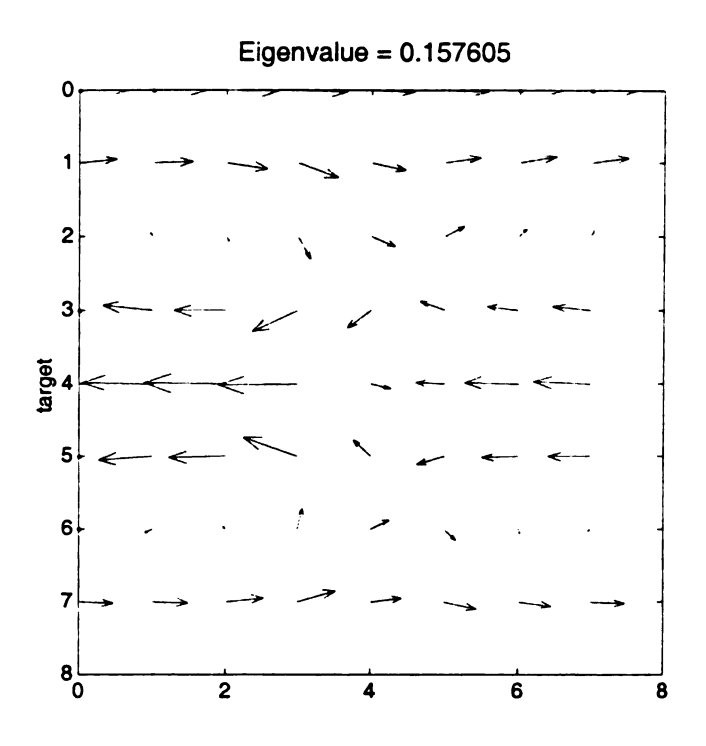


Figure 4.16 6th Mode shape from the target stiffness matrix

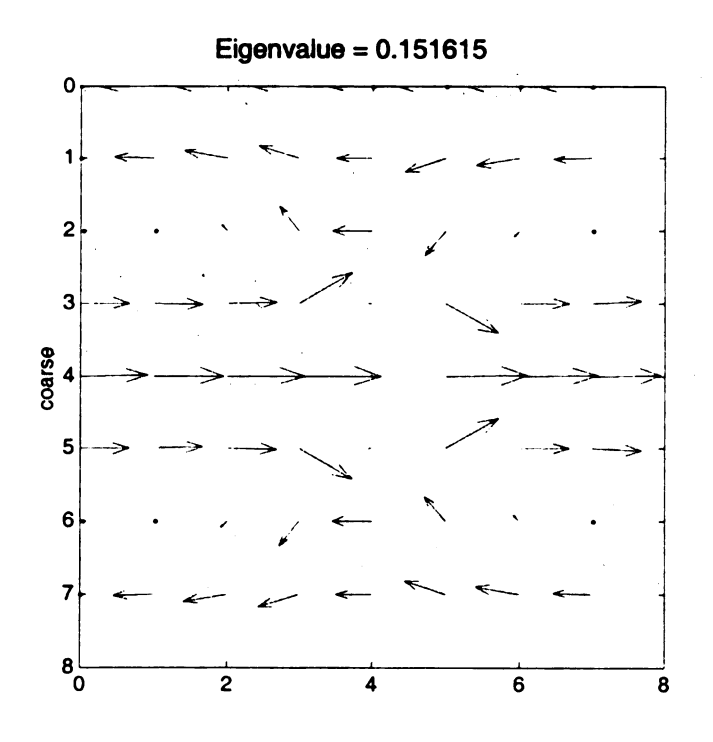


Figure 4.17 10th Mode shape for the coarse material distribution

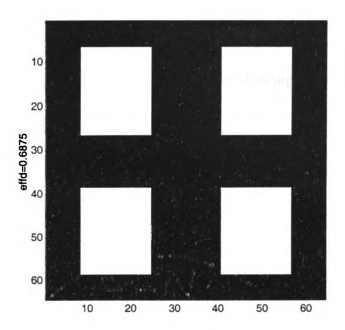


Figure 4.18 Fine scale material distribution

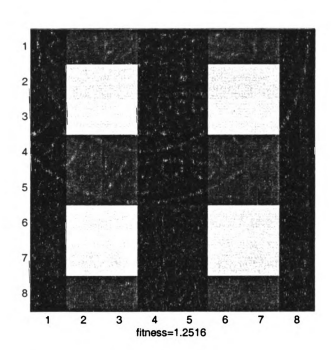


Figure 4.19 Coarse scale material solution

The second scale results also yield interesting solutions; this can be seen in the figures above. As seen in the solutions the use of gray material becomes more apparent and necessary. Also in general, lower mode shapes are taken into account for the higher scale materials. Again the mode shapes are inspected showing good results.

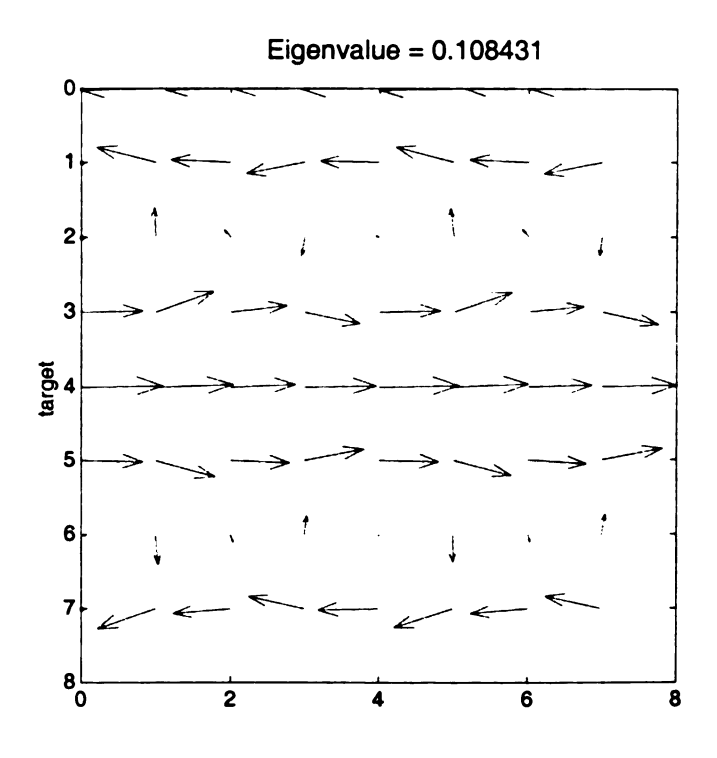


Figure 4.20 3rd Mode shape from the target stiffness matrix

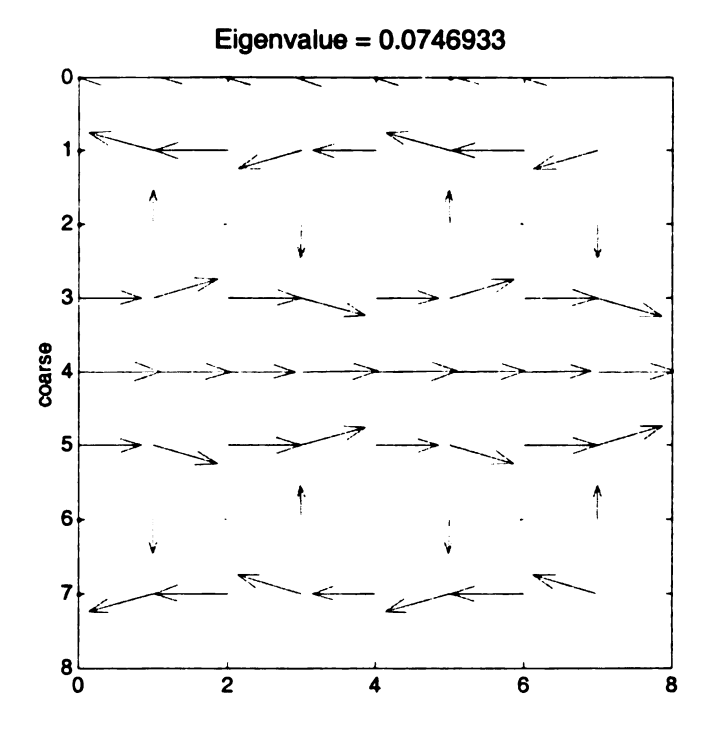


Figure 4.21 4th Mode shape for the coarse material distribution

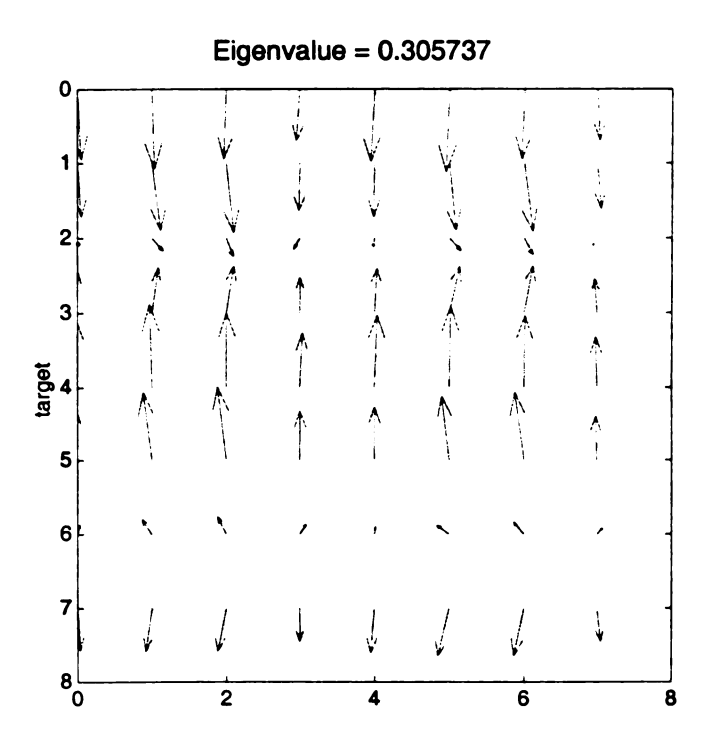


Figure 4.22 10th Mode shape from the target stiffness matrix

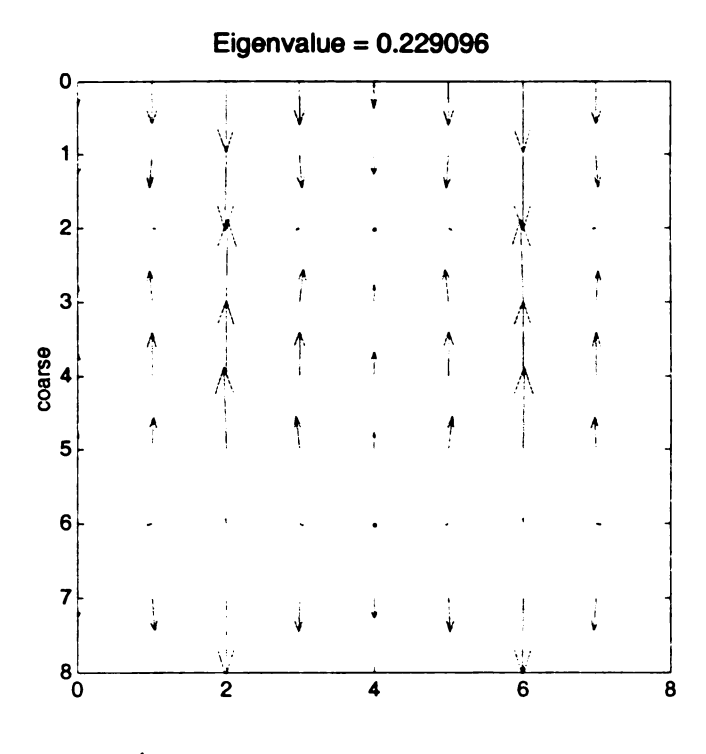


Figure 4.23 15th Mode shape for the coarse material distribution

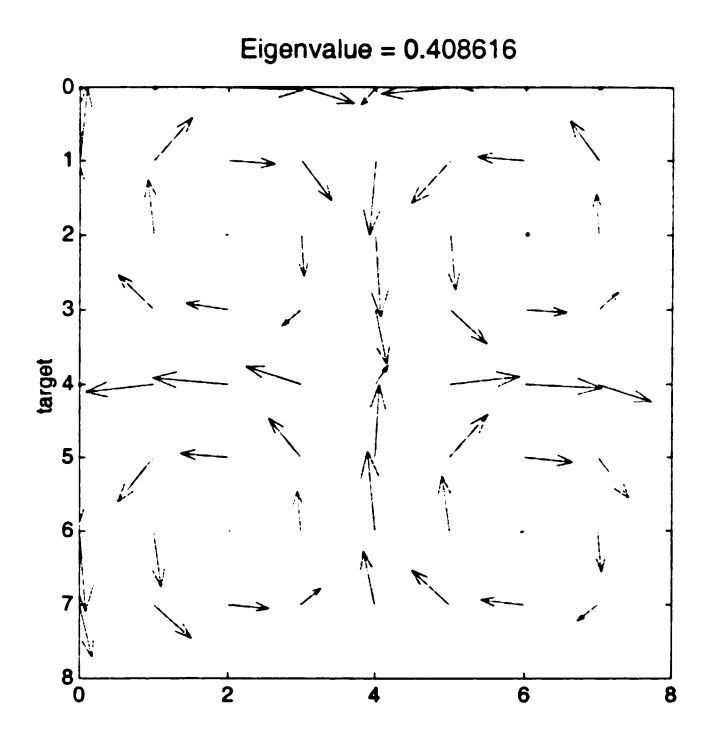


Figure 4.24 12th Mode shape from the target stiffness matrix

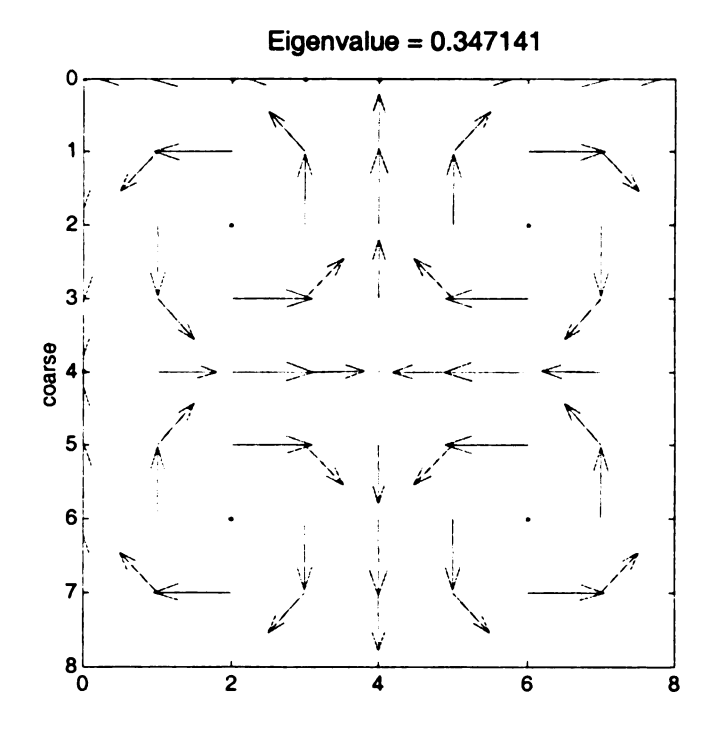


Figure 4.25 21st Mode shape for the coarse material distribution

The figures above showed one common trend: the target matrix was always stiffer than the coarse scale material distribution. This problem can be solved by scaling up the values in the coarse scale material.

Looking at another example from scale 2, again noticing the energy similarity in the mode shapes.

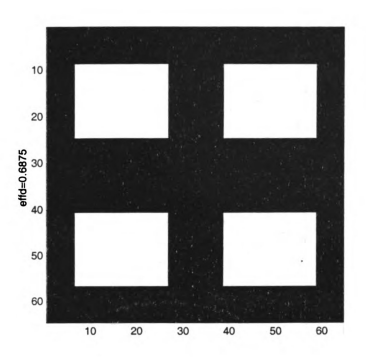


Figure 4.26 Fine scale material distribution

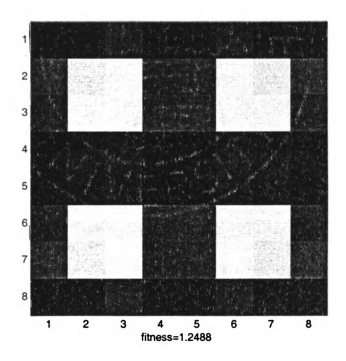


Figure 4.27 Coarse scale material distribution solution

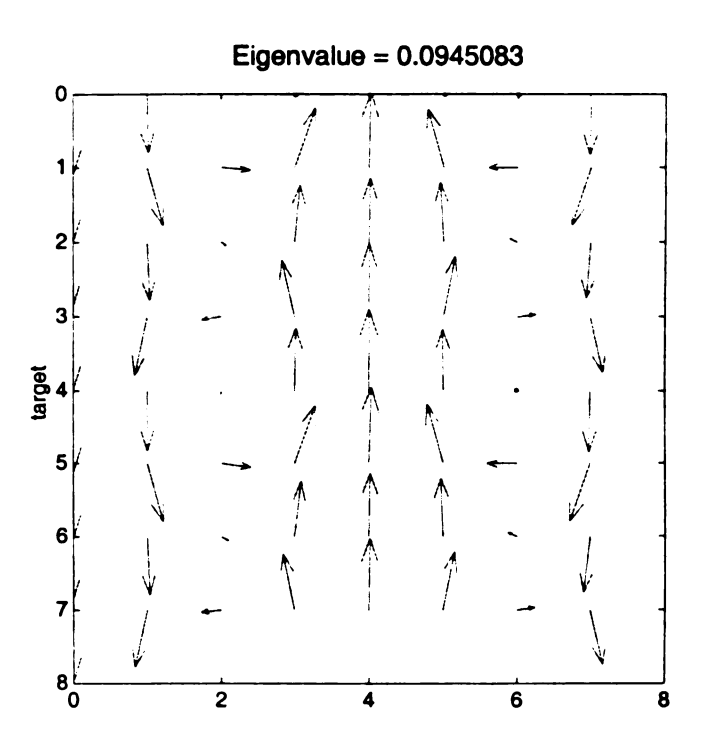


Figure 4.28 3rd Mode shape from the target stiffness matrix

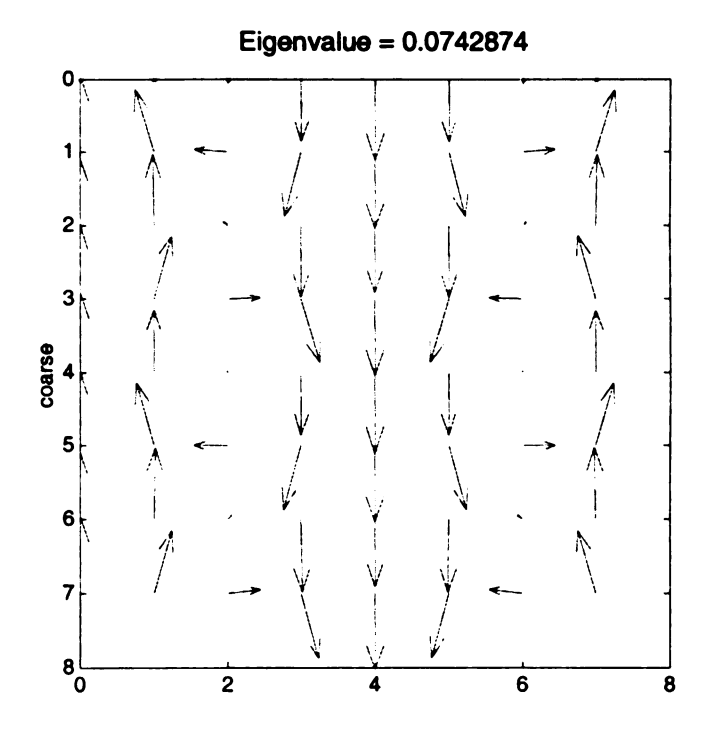


Figure 4.29 4th Mode shape for the coarse material distribution

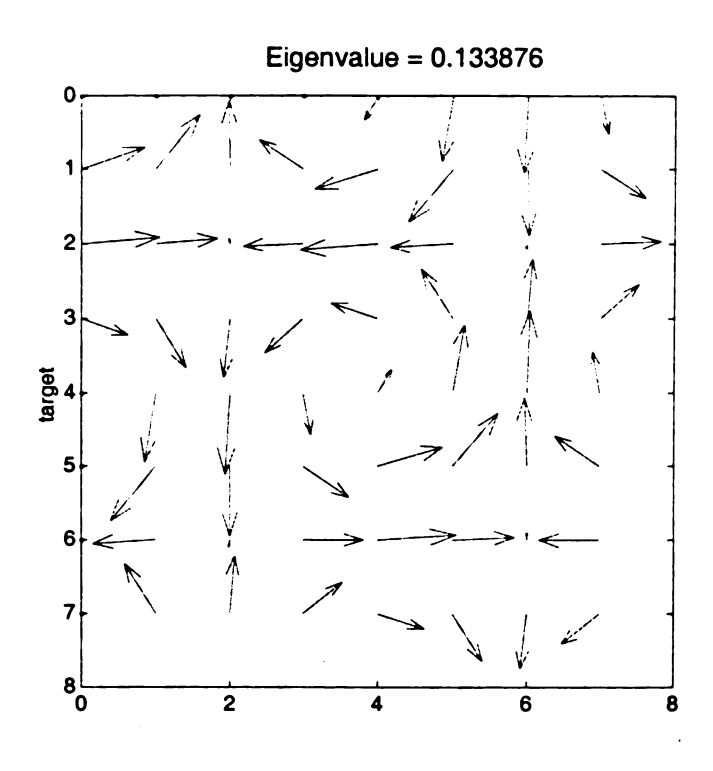


Figure 4.30 5th Mode shape from the target stiffness matrix

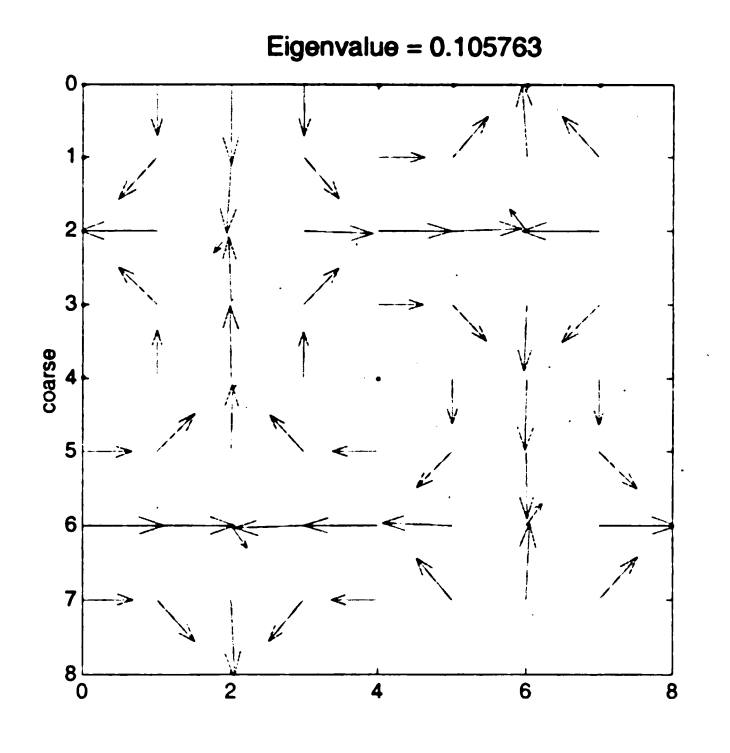


Figure 4.31 5th Mode shape for the coarse material distribution

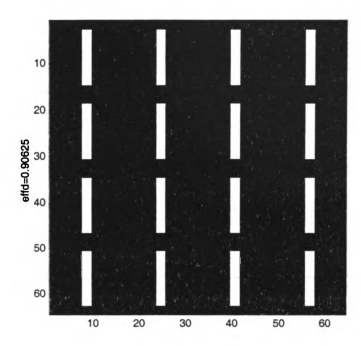


Figure 4.32 Fine scale material distribution

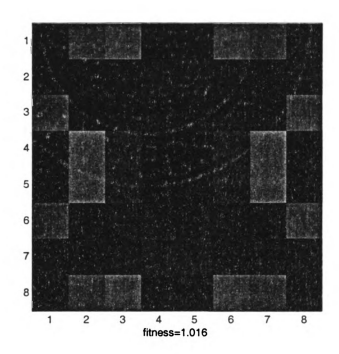


Figure 4.33 Coarse scale material distribution solution

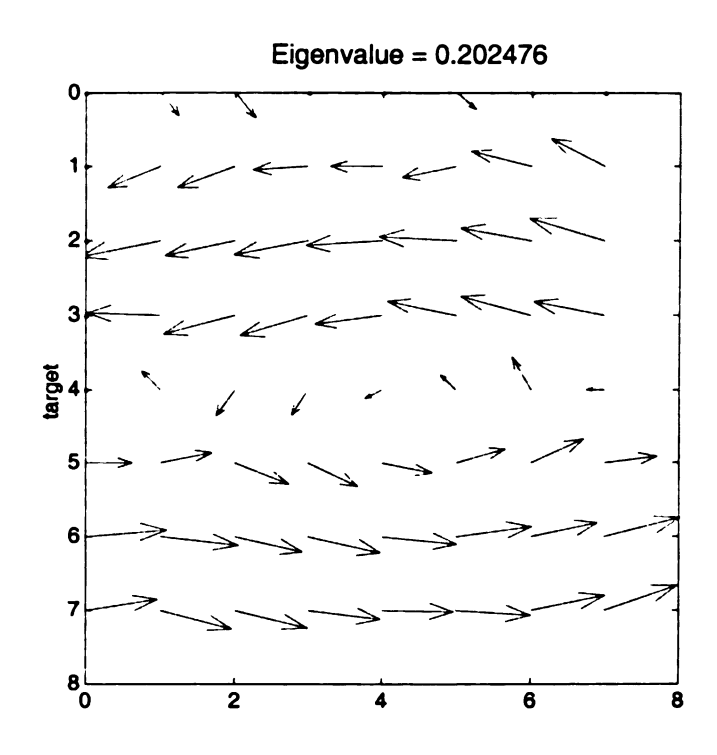


Figure 4.34 4th Mode shape from the target stiffness matrix

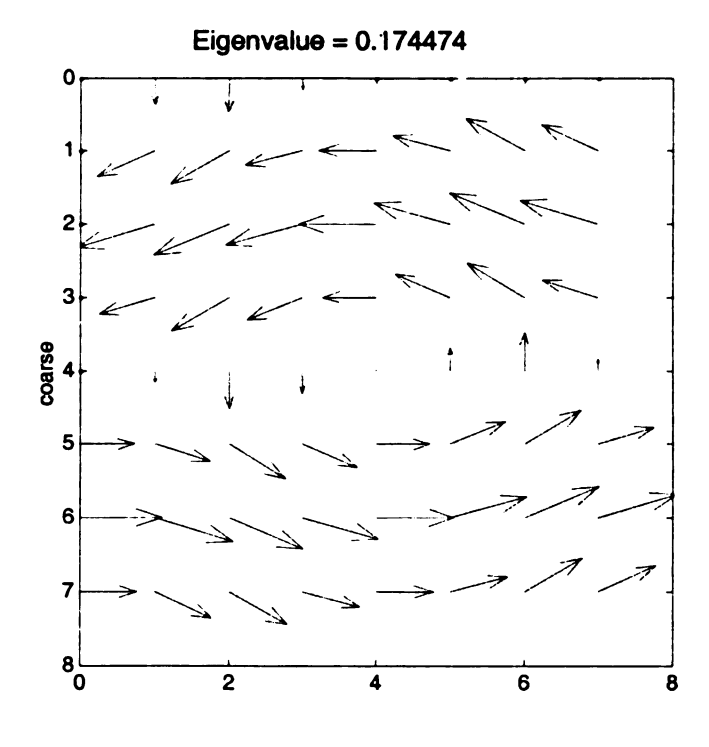


Figure 4.35 3rd Mode shape for the coarse material distribution

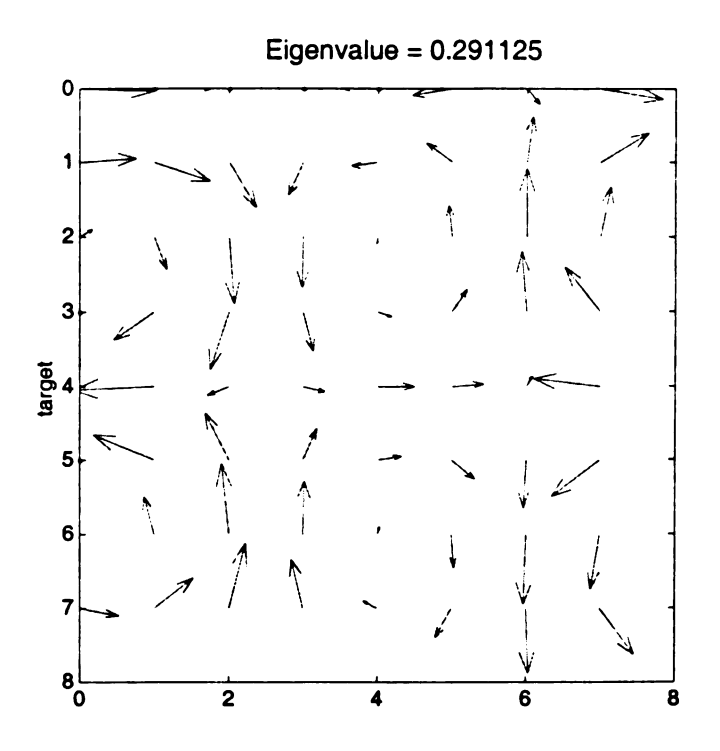


Figure 4.36 7th Mode shape from the target stiffness matrix

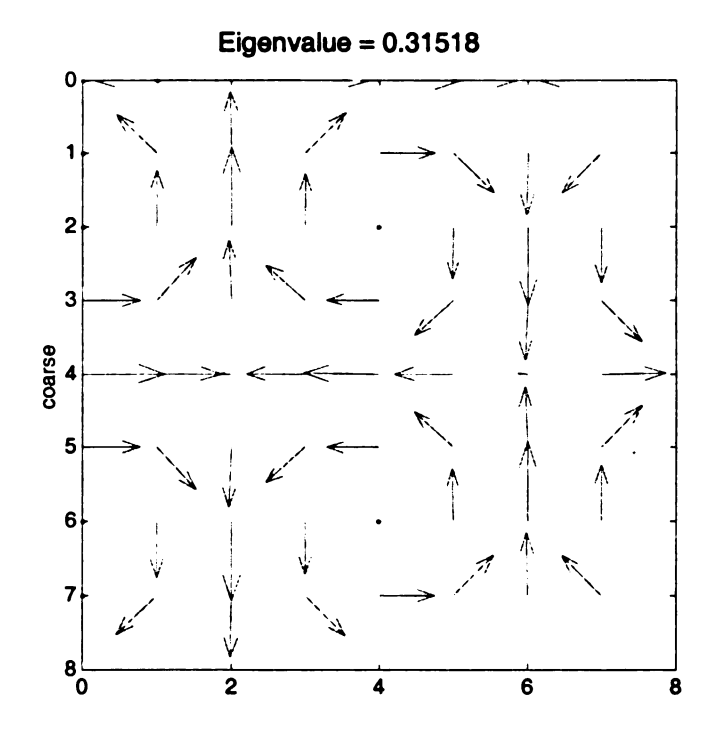


Figure 4.37 7th Mode shape for the coarse material distribution

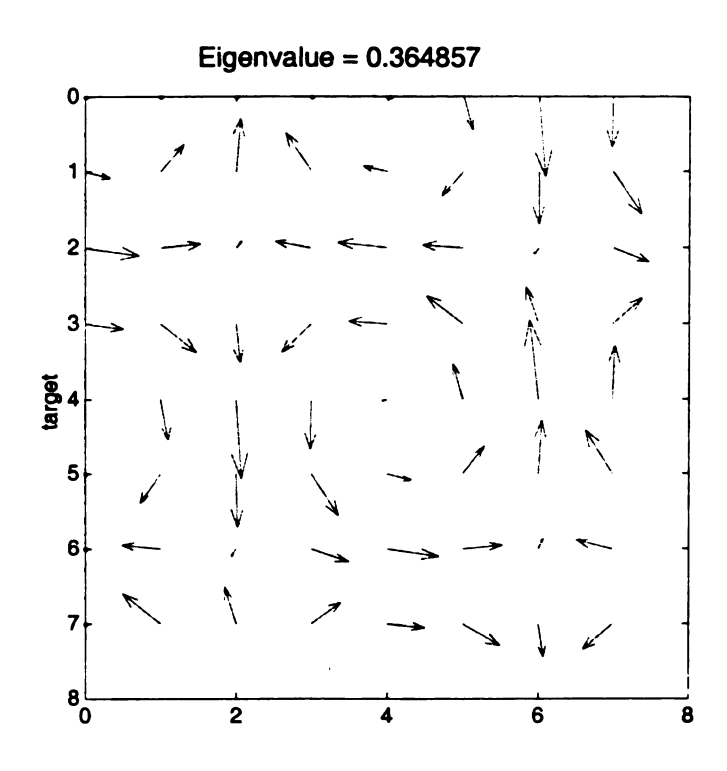


Figure 4.38 9th Mode shape from the target stiffness matrix

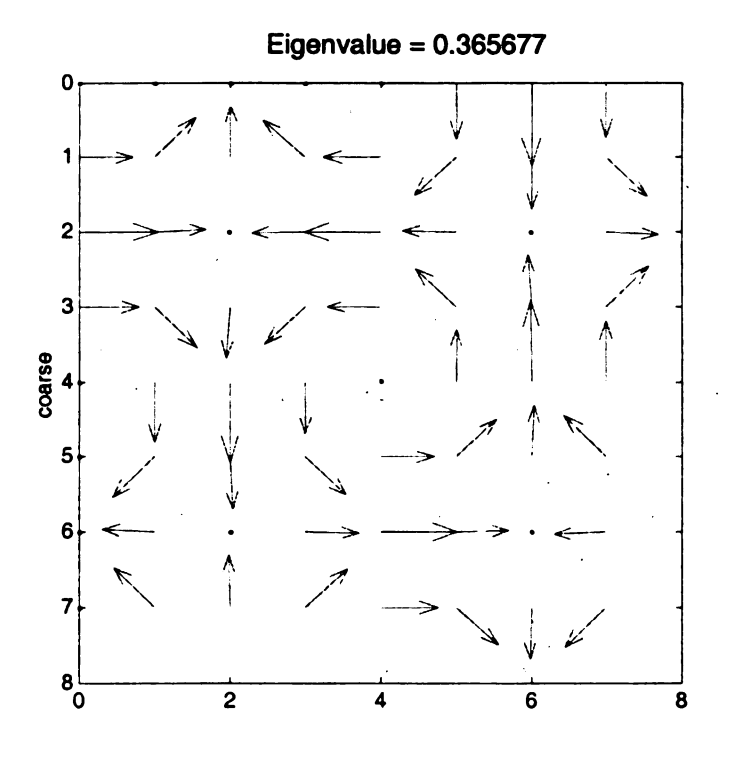


Figure 4.39 9th Mode shape for the coarse material distribution

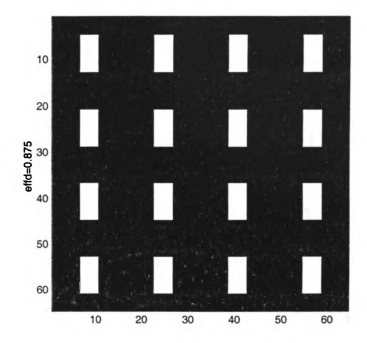


Figure 4.40 Fine scale material distribution

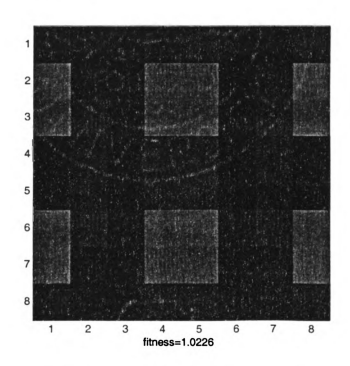


Figure 4.41 Coarse scale material solution

Again looking at the eigenvectors of the two systems and comparing the eigenvalues.

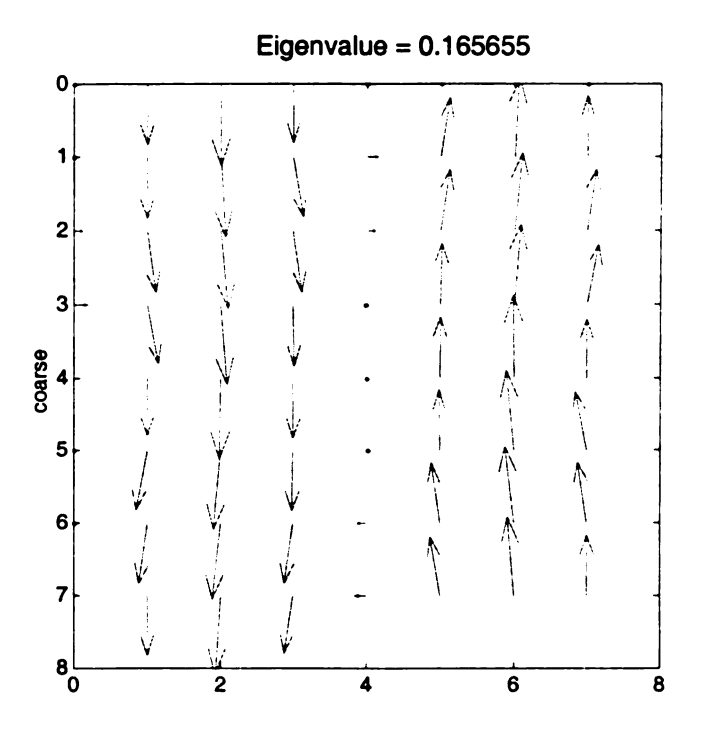


Figure 4.42 3rd Mode shape from the target stiffness matrix

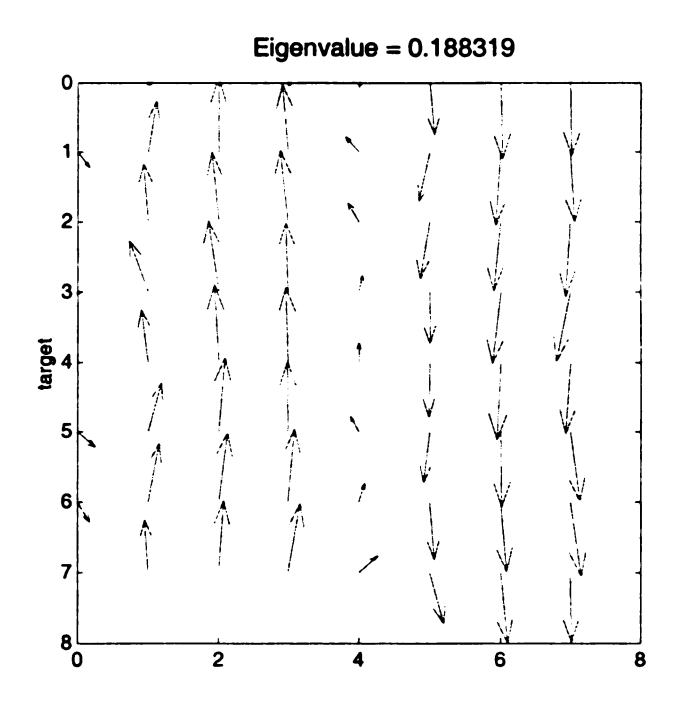


Figure 4.43 4th Mode shape for the coarse material distribution

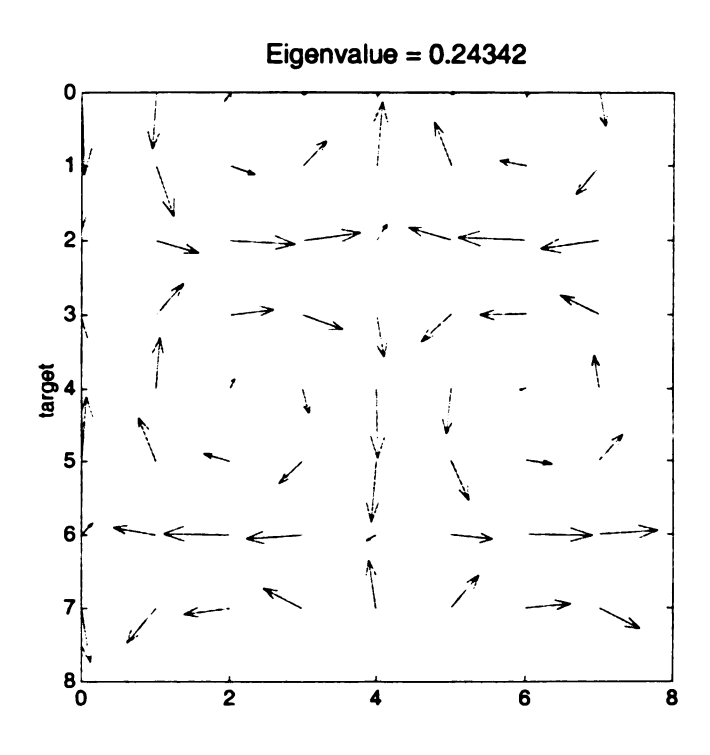


Figure 4.44 5th Mode shape from the target stiffness matrix

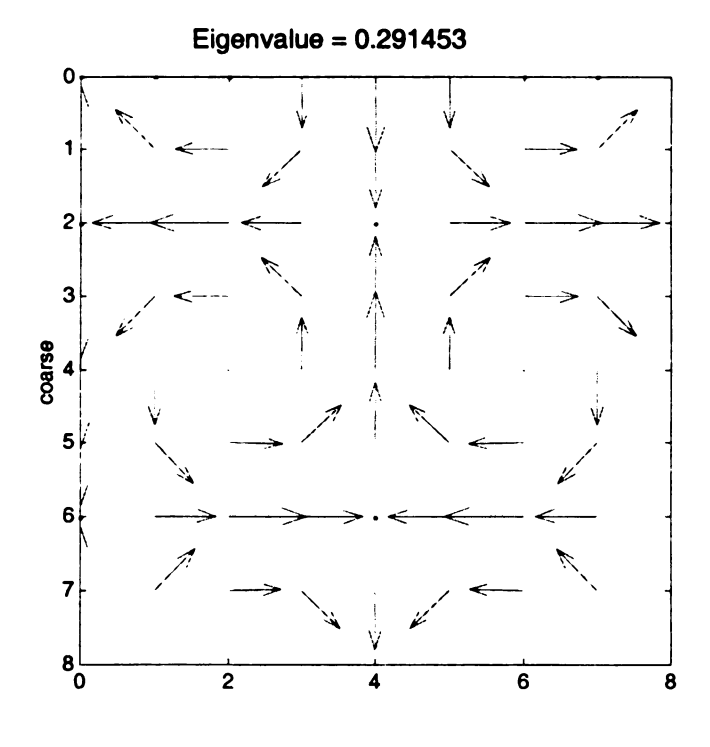


Figure 4.45 7th Mode shape for the coarse material distribution

As shown in the figures for the third scale the use of gray material is increased from the second scale. The eigenvectors taken into account start with the 3rd mode shape. As stated before, this is the first non-rigid body mode shape.

This chapter presented fine scale material distributions along with the coarse scale material solutions. These solutions had varying success, which can be seen by comparing the energies associated with the modes shapes for the solutions. The last chapter is going to discuss the conclusions of this research.

Chapter 5

CONCLUSIONS

A model order reduction technique was shown. This technique uses a multi-resolution analysis on a non-homogenous material distribution with fine scale features to construct a wavelet based reduced stiffness matrix. A Equivalent material problem was posed; find a material distribution that represents a reduced wavelet stiffness matrix. This problem was successfully solved using a genetic algorithm.

Results for three different scales are shown along with mode shapes of the reduced matrix and the coarse scale material solution. These mode shapes were matched, and then the energy (eigenvalues) compared. If the energy between the two systems were equal it could be said that the fine scale material distribution could be represented by the coarse scale solution for that frequency. This fact has been shown with good accuracy that this procedure can be done not for just one frequency, but a range of frequencies, making this correlation between the fine scale and the coarse scale correct for a wide range of loading conditions.

Acknowledgement

This work was supported, in part, by the National Science Foundation through grant DMI9912520. This support is gratefully acknowledged

Reference

- [1] A.R. Diaz, 1999, Int. Journal of Numerical Methods in Engineering, 44 1599-1616. A Wavelet Galkerin Scheme for Analysis of Large Scale Problems on Simple Domains
- [2] M. I. Friswell., J.E.T. Penny and S.D. Garvey, 1995 Mechanical Systems and Signal Processing 9, 317-328. Using Linear Modeling Reduction Techniques To Investigate The Dynamics of Structures With Local Non-Linearities
- [3] R J GUYAN, 1965 0854 AIAA Journal 3 279 Reduction of stiffness and mass matrices
- [4] S. Chellappa and A.R. Diaz, 2002 Fifth World Congress on Computational Mechanics, Vienna, Austria, July 7-12. A Multi-Resolution Reduction Scheme for Structural Optimization.
- [5] M. Paz 1984 AIAA Journal 22, 724-727. Dynamic Condensation.
- [6] J.C. O'Callahan 1989 Proceedings of the 7th International Modal Anaylsis Conference, Las Vegas,17-21. A procedure for an improved reduced system (IRS) model.
- [7] M. I. Friswell., J.E.T. Penny and S.D. Garvey, 1998 Journal of Sound and Vibration 211, 123-132. The convergence of the iterated IRS method
- [8] Sigmund, O. 1994 International Journal of Solids and Structures 31, 2312-2329. Materials with prescribed constitutive parameters: an inverse homogenization problem.
- [9] Sigmund, O.: Tailoring Materials with Prescribed Elastic Properties. Mechanics of Materials, Vol. 20, pp. 351-368, 1995.
- [10] Sigmund, O. and Torquato, S.: Composites with Extremal Thermal Expansion Coefficients. Applied Physics Letters, Vol. 69, No. 21, pp. 3203-3205, 1996.
- [11] OU W. 2001 Tailoring Materials with Prescribed Constitutive Parameters using Polygonal Cells. Thesis submitted to Michigan State University College of Engineering.
- [12] Zalzala, A.M.S and Fleming P.J. 1997 Genetic Algorithms in engineering systems
- [13] Buckles B. and Petry, F. 1992. Genetic Algorithms

- [14] Houck, C. and Joines, J. and Kay, M. 1996 A Genetic Algorithms for Function Optimization: A Matlab Implentation
- [15] www.geatbx.com/links/ea_matlab.html
- [16] Sigmund, O. and Torquato, S. Journal of Smart Media and Structures: Design of smart materials using topology optimization vol8 1999

